Injection Rates—The Effect of Mobility Ratio, Area Swept, and Pattern

JOHN C. DEPPE
MEMBER AIME

THE ATLANTIC REFINING CO.
DALLAS, TEX.

ABSTRACT

A method is presented for calculating approximate injection rates in secondary recovery operations. The method can be applied to cases of unequal fluid mobilities, irregular well patterns and boundary patterns.

The steady-state pressure distributions for the four flood patterns reported by Muskat and for five additional patterns reveal that most of the difference in pressure between the injection and producing wells occurs in regions around the wells which can adequately be described as regions of radial flow. This leads to a method of calculating injectivity by approximating the flood pattern with radial flow elements (or a combination of radial- and linear-flow elements for some patterns such as the direct line drive). Irregular and boundary patterns can also be approximated by radial and linear elements.

Each of these elements can be described by radial- and linear-flow equations and the results combined as series flow resistances to give an approximate equation for the initial injection rate. The mobility ratio does not affect the initial rate; therefore, if the well pattern is one of those regular patterns for which theoretical rate equations have been derived for unity mobility ratio, the approximate initial rate equation can be improved by adjusting it to match the theoretical equation. The available theoretical rate equations are listed, including five new cases.

As the flood progresses, the injectivity changes because in general the flood front will divide the pattern into areas of different fluid mobilities. Simple shapes can be assumed for the flood front so that both areas can be divided into radial- and linear-flow elements.

Radial- and linear-flow equations are applied to these elements to account for the change in flow resistance behind the front.

To calculate injection rates after breakthrough, it is necessary to know the sweep efficiency at breakthrough. Areal sweep data are available in the literature for a number of patterns, and sufficiently accurate breakthrough sweep efficiency can be estimated from these data if it is not otherwise available.

Again, simple shapes for the flood front can be assumed after breakthrough, and injection rates can be calculated for the remainder of the flood. When areal sweep data are available, these data can be used to check the calculated injection rates after breakthrough.

Injection rates calculated by this approximate method compare favorably with available model data.

INTRODUCTION

When the fluid mobilities in the swept and unswept regions are equal, the injectivity will not change as the flood front advances; and for regular patterns it can be calculated by mathematical formulas.[1]

When the fluid mobilities in the swept and unswept regions are not equal, the injectivity will increase or decrease as the flood front advances. In this case, the injectivity has not been calculated by analytical means for any practical well pattern; and, furthermore, scale model[5] and analog[4,6] results have been published only for the five-spot pattern.

The main object of this paper is to present an approximate method for calculating injectivity for the case of unequal mobilities. The method can be applied to regular, irregular and boundary patterns.

Before the approximate method is discussed, the analytical formulas for equal mobilities will be summarized, and the analytical solution for radial flow with unequal mobilities will be used to show how the injectivity changes as the flood progresses.

EQUAL MOBILITIES, REGULAR PATTERNS

In a flooding operation the injectivity, the rate at which fluid can be injected per unit difference in pressure between injection and producing wells, depends on basic physical properties and, in addition, on three variables to be treated here—the area of the swept region, the fluid mobilities in the swept and unswept regions, and the well geometry (pattern,

SPE 1472-G

[1]References given at end of paper.

spacing and wellbore radii).

When the fluid mobilities in the swept and unswept regions are the same, the injectivity of a given well array is independent of the first variable, the size and shape of the area swept, and is directly proportional to the single fluid mobility involved. The calculation of the injectivity thus reduces to the geometrical problem of treating the particular well pattern, well spacing and well radii.

For regular patterns, Muskat[1] has offered a method for finding analytical mathematical solutions and has worked out the formulas for special cases — the direct line drive, the staggered line drive, the five-spot and the seven-spot. Five more cases are presented here—the nine-spot with arbitrary corner-well to side-well producing ratios, a direct-line-drive boundary pattern, two five-spot boundary patterns and a nine-spot boundary pattern. These nine cases are listed in Table 1, which is thus a summary of the available results on injectivity of regular patterns with unity mobility ratio. The derivations of the five new cases are omitted because they follow the method of Muskat.

The five new cases can be used in the development of an approximate method for handling irregular patterns. The nine-spot will be used to show the extent of approximately radial flow even for large differences in corner-well and side-well rates. The four boundary cases can be used to aid in estimating the angle open to flow in irregular-boundary patterns.

RADIAL SYSTEM, UNEQUAL MOBILITIES

In each of the cases appearing in Table 1, the

injectivity is independent of the area swept and depends on mobility only to the extent of simple proportionality. The only important variable is the

TABLE 1B — INJECTIVITIES FOR REGULAR PATTERNS WITH UNITY MOBILITY RATIO.

NINE-SPOT[2]

$$i = \frac{0.001538 \, \lambda h \Delta P_{i,c}}{\frac{1+R}{2+R} \left[\log \frac{d}{r_w} - 0.1183 \right]},$$

$$i = \frac{0.003076 \, \lambda h \Delta P_{i,s}}{\frac{3+R}{2+R} \left[\log \frac{d}{r_w} - 0.1183 \right] - \frac{0.301}{2+R}},$$

R = Ratio of producing rates of corner well (c) to side well (s),

$\Delta P_{i,c}$ = Difference in pressure between injection well and corner well (c),

$\Delta P_{i,s}$ = Difference in pressure between injection well and side well (s).

DIRECT LINE DRIVE BOUNDARY PATTERN[2]

$$i = \frac{0.003076 \, \lambda h \Delta P_{i1',q1'}}{\frac{q_1 + 4q_1'}{q_1 + 2q_1'} \left[\log \frac{d}{r_w} + 0.166 + 0.400R \right] + \frac{1.368 q_1 (1+R)}{q_1 + 2q_1'}},$$

$$R = \frac{q_2}{q_1} = \frac{q_2'}{q_1'},$$

$\Delta P_{i1',q1'}$ = Difference in pressure between injection well i_1' and producing well q_1'.

RESERVOIR BOUNDARY

TABLE 1C — INJECTIVITIES FOR REGULAR PATTERNS WITH UNITY MOBILITY RATIO.

FIVE-SPOT BOUNDARY PATTERN[2]

$$i' = \frac{0.001538 \, \lambda h \Delta P_{i',q'}}{\log \frac{d}{r_w} - 0.158 - 0.036 \frac{q}{q'}},$$

RESERVOIR BOUNDARY

$\Delta P_{i',q'}$ = Difference in pressure between injection well i' and producing well q'

(Wells of outer row are alternating injection and producing wells.)

FIVE-SPOT BOUNDARY PATTERN[2]

$$i' = \frac{0.003076 \, h\lambda \, (q_1 + q_2 + 2q_1' + 2q_2') \, \Delta Pi', q_1'}{2q_1' \left[(3+R)(\log \frac{d}{r_w} + 0.815) - 1.7216 \right] + q_1(1+R)(\log \frac{d}{r_w} - 0.098)},$$

$$R = \frac{q_2}{q_1} = \frac{q_2'}{q_1'}$$

RESERVOIR BOUNDARY

$\Delta P_{i',q'}$ = Difference in pressure between injection well i' and producing well q'.

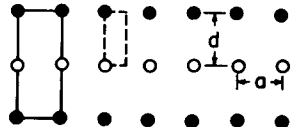(Wells of outer row are all producing wells.)

TABLE 1A — INJECTIVITIES FOR REGULAR PATTERNS WITH UNITY MOBILITY RATIO.

Solid line indicates symmetry pattern of infinite well network.
Dashed line indicates symmetry element of infinite well network.
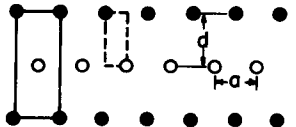
Code: O Injection Wells, ● Producing Wells

DIRECT LINE DRIVE[1]

$$i = \frac{0.001538 \, \lambda h \Delta P}{\log \frac{a}{r_w} + 0.682 \frac{d}{a} - 0.798}$$
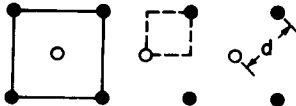
$$\frac{d}{a} \geq 1$$
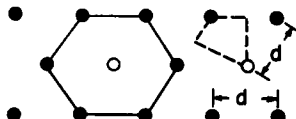
STAGGERED LINE DRIVE[1]

$$i = \frac{0.001538 \, \lambda h \Delta P}{\log \frac{a}{r_w} + 0.682 \frac{d}{a} - 0.798}$$

$$\frac{d}{a} \geq 1$$

FIVE-SPOT[1]

$$i = \frac{0.001538 \, \lambda h \Delta P}{\log \frac{d}{r_w} - 0.2688}$$
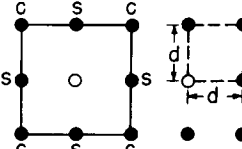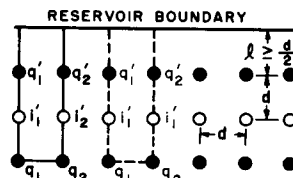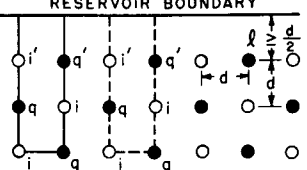
SEVEN-SPOT[1]

$$i = \frac{0.002051 \, \lambda h \Delta P}{\log \frac{d}{r_w} - 0.2472}$$

TABLE 1D — INJECTIVITIES FOR REGULAR PATTERNS WITH UNITY MOBILITY RATIO.

NINE-SPOT BOUNDARY PATTERN[2]
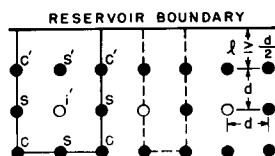
$$i' = \frac{0.003076 \, \lambda h \Delta P_{i',\,s'}(2q_s' + 2q_c' + 3q_s + q_c)}{2q_s'\left[(2+R)\{\log\frac{d}{r_w} + 0.548\} - 1.49\right] + q_s\left[(3+R)\{\log\frac{d}{r_w} + 0.885\} - 0.577\right]},$$

$$i' = \frac{0.003076 \, \lambda h \Delta P_{i',\,c'}(2q_s' + 2q_c' + 3q_s + q_c)}{2q_s'\left[(1+2R)\{\log\frac{d}{r_w} + 0.204\} + 0.362\right] + q_s\left[(3+R)\{\log\frac{d}{r_w} - 0.460\} + 0.124\right]},$$

$$R = \frac{q_c}{q_s} = \frac{q_c'}{q_s'},$$

$\Delta P_{i',\,s'}$ = Difference in pressure between injection well i' and producing well s'.

$\Delta P_{i',\,c'}$ = Difference in pressure between injection well i' and producing well c'.

RESERVOIR BOUNDARY

system geometry and, for these restricted conditions, analytical solutions are possible.

In this section another analytical solution is considered, this time made possible by geometrical simplicity. This solution illustrates the manner in which the other variables enter the problem, showing explicitly the variation of injectivity with position of the flood front for any mobility ratio.

Consider a radial system with a central injection well of radius r_w and imagine that fluid is produced uniformly from each point on a circle of radius r_e. Purely radial flow will result, and the front between injected and original fluids will be a circle whose radius will be called r_f. Simple radial-flow equations will apply in both the swept and unswept regions. In the unswept region, the production rate q will be given by

$$q = \frac{0.003076 \, h\lambda_u \, (p_e - p_f)}{\log(r_e/r_f)}, \dots\text{res B/D}$$

$$\dots\dots\dots\dots\dots\dots\dots\dots (1)$$

where h is the thickness (in feet), λ_u is the fluid mobility in the unswept region (millidarcies/centipoise), and p_e and p_f are the pressures at the outer boundary and at the front (psi). Similarly, in the swept region the injection rate i will be

$$i = \frac{0.003076 \, h\lambda_s \, (p_f - p_w)}{\log(r_f/r_w)}, \dots\text{res B/D}$$

$$\dots\dots\dots\dots\dots\dots\dots\dots (2)$$

where λ_s is the mobility in the swept region and p_w is the pressure at the injection well.

For steady-state incompressible flow, the injection rate is equal to the production rate ($i = q$), and these two equations can be combined to eliminate p_f and give an expression for the injection rate in terms of the position of the front r_f which is valid

for any mobility ratio.

$$i = \frac{0.003076 \, h\lambda_u \Delta p}{\log\dfrac{r_e}{r_f} + \dfrac{1}{M}\log\dfrac{r_f}{r_w}}, \dots\text{res B/D}$$

$$\dots\dots\dots\dots\dots\dots\dots\dots (3)$$

where $\Delta p = p_e - p_w$ and $M = \lambda_s/\lambda_u$.

In most applications, it is convenient to express the variation in injectivity with the progress of the front in terms of the initial injectivity. In this case, that is, a relative injectivity I_r is defined as the ratio of the injectivity at any time (given by Eq. 3) to the initial injectivity (given by Eq. 3 with $r_f = r_w$).

$$I_r = \frac{\log\dfrac{r_e}{r_w}}{\log\dfrac{r_e}{r_f} + \dfrac{1}{M}\log\dfrac{r_f}{r_w}} \dots\dots\dots (3a)$$

The relative injectivity starts at unity when $r_f = r_w$ and ends at M when $r_f = r_e$ (corresponding to complete sweeping of the area and complete change of fluid mobility from λ_u to λ_s).

Curves calculated from this equation are plotted in Fig. 1 for mobility ratios of 5, 1 and 1/2, and for radius ratios r_e/r_w of 160 and 500. These ratios also appear in later comparisons of approximate
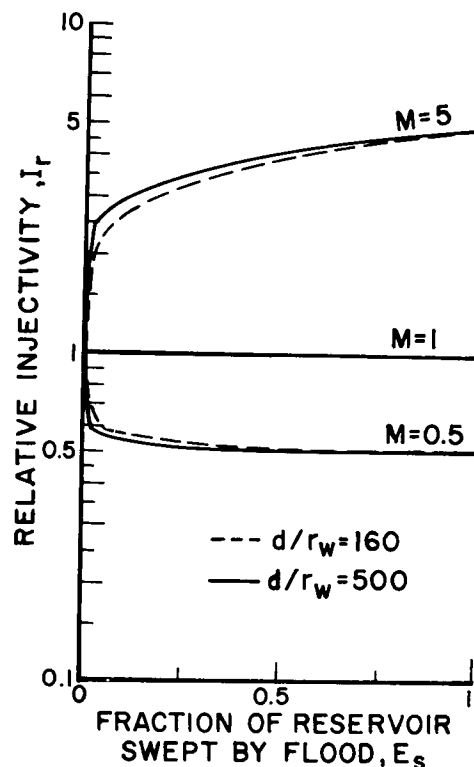
FIG. 1 — EFFECT OF MOBILITY RATIO ON RELATIVE INJECTIVITY DURING SWEEPOUT OF RADIAL FLOOD PATTERN. CALCULATED FROM EQ. 3a.

calculations and model results. The relative injectivity is plotted against fraction of area swept E_s, rather than against the position of the front. In this case, the relation is $r_f^2/r_e^2 = E_s$, for $r_w \ll r_e$.

The relative injectivity changes very rapidly during the early part of the flood, and then shows a gradual change during the remainder of the flood. This early, rapid change followed by a long period of slow change is typical of radial systems. In complex systems, the rapid change occurs while the flood front is moving out from the injection well in a near-radial manner.

In this simple example of complete radial flow, the period of gradual change extends to the end of the operation because breakthrough of the injected fluid into the producing circle occurs at complete sweep of the area. In a more complex system, with producing wells rather than the producing circle, a nose of injected fluid may reach a producing well before complete sweep of the area. After this breakthrough point, there again will be a more rapid change in the injectivity.

APPROXIMATE METHOD

REGULAR PATTERNS

Analytical equations of steady-state pressure distributions in complex flood patterns have been derived by Muskat[1] for the case of unity mobility ratio. An examination of these pressure distributions shows that most of the pressure difference between injection wells and producing wells occurs in areas around the wells which can adequately be described as regions of radial flow. In flood patterns as complex as the nine-spot pattern (see the Appendix), these regions of near-radial flow still occur around the injection and producing wells.

Porous, fluid-flow model studies[3] show that, even when the mobilities of the swept and unswept regions are different, the flood front moves out from the injection well in a radial manner during the early part of the flood.

These properties of flood systems suggest that the injectivity of any system can be simply and quickly approximated by dividing the pattern into segments of radial and linear flow and computing the total flow by combining the radial- and linear-flow equations which apply to individual segments.

In estimating injectivity by this approximate method, the volume of the pattern must be divided among the producing wells of the pattern. The volume assigned to each of the wells is then approximated by regions of radial and linear flow. The injectivity can be calculated by assuming that the flood front advances radially in the radial regions and linearly in the linear regions until breakthrough is approached. In this manner, injectivity prior to breakthrough of the swept region into a producing well can be estimated without the need of areal-sweepout data for the flood pattern.

As breakthrough is approached, a nose begins to grow at the flood front and streaks to the producing well during a short period of time when only a small part of the total-pattern volume is swept. As further production occurs, the finger opens up and the rate of flow from the swept region is nearly proportional to the angle this finger makes at the producing well. Prats, et al,[6] showed that it is the existing angle open to flow which controls the injectivity. For a given angle, the exact shape of the flood front after breakthrough has little effect on injectivity. If the flood front after breakthrough is approximated by a circle with a sector whose angle is proportional to the rate of flow from the swept region, the injectivity after breakthrough can be estimated from the same radial- and linear-flow segments used before breakthrough.

To illustrate this method of estimating injectivity, consider the five-spot pattern shown in Table 1. The symmetry element of the five-spot can be divided into two radial segments as shown in Fig. 2.

Applying the radial-flow equation to each of the two radial segments and combining gives for the *initial* injection rate

$$i = \frac{0.003076 \, h\lambda_u \, (p_{wi} - p_{wp})}{\log \dfrac{r_{ei}}{r_{wi}} + \log \dfrac{r_{ep}}{r_{wp}}} \, ,...\text{res B/D}$$

$$\cdots \cdots \cdots \cdots \cdots \cdots \cdots \cdots (4)$$

where h = net pay thickness, ft,

r_{ei} = radius of the radial segment around the injection well,

r_{ep} = radius of the radial segment around the producing well,

r_{wi} = effective wellbore radius of the injection well,

r_{wp} = effective wellbore radius of the producing well,

p_{wi} = pressure at injection well, psi,

p_{wp} = pressure at producing well, psi,

λ_u = mobility of the reservoir fluid, k_u/μ_u, md/cp, and

d = distance between injection and producing wells (see Fig. 2).

When the effective wellbore radii are equal and $r_{ei} = r_{ep}$, Eq. 4 becomes

$$i = \frac{0.001538 \, h\lambda_u \, (p_{wi} - p_{wp})}{\log \dfrac{d}{r_w} - 0.249} \, ,...\text{res B/D}$$

$$\cdots \cdots \cdots \cdots \cdots \cdots \cdots \cdots (5)$$
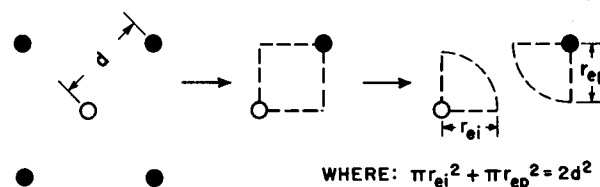

WHERE: $\pi r_{ei}^2 + \pi r_{ep}^2 = 2d^2$

FIG. 2 — DIVISION OF FIVE-SPOT PATTERN AREA INTO APPROXIMATING RADIAL-FLOW SECTORS FOR DERIVING APPROXIMATE EQUATION OF INJECTIVITY.

which agrees very closely with the exact equation for the five-spot pattern given in Table 1 (the only difference is between the constants 0.249 and 0.269). A still closer agreement could be obtained by approximating the pattern area with a linear-flow segment between two radial-flow segments.

On the assumption that the flood front moves out in a true radial manner, the injectivity while the front is between the injection well and the radial boundary r_{ei} is

$$R_6 = \frac{1}{M} \log \frac{r_f}{r_{wi}} + \log \frac{r_{ei}}{r_f}$$

$$+ \log \frac{r_{ep}}{r_{wp}}$$

$$\frac{i}{p_{wi} - p_{wp}} = \frac{0.003076 \, h\lambda_u}{R_6} ,$$

$$\text{res B/D-psi}$$

$$\quad\quad\quad\quad\quad\quad\quad\quad\quad\quad\quad (6)$$

where M = mobility ratio λ_s/λ_u, and the relation between the radius of the flood front r_f, and the fraction of total area covered by the swept region E_s, is

$$r_f = d \sqrt{\frac{2E_s}{\pi}} . \quad \text{ft} \quad\cdots\cdots (7)$$

When the flood front is between the boundary r_{ep} and the producing well prior to breakthrough, the injectivity is

$$R_8 = \frac{1}{M} \log \frac{r_{ei}}{r_{wi}} + \frac{1}{M} \log \frac{r_{ep}}{r_f}$$

$$+ \log \frac{r_f}{r_{wp}}$$

$$\frac{i}{p_{wi} - p_{wp}} = \frac{0.003076 \, h\lambda_u}{R_8} ,$$

$$\text{res B/D-psi}$$
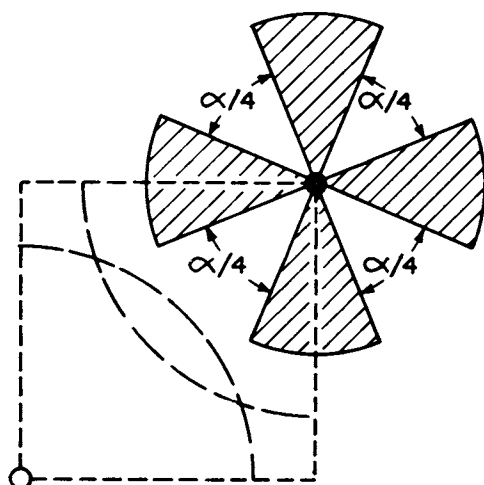
$$\quad\quad\quad\quad\quad\quad\quad\quad\quad\quad\quad (8)$$

FIG. 3 —ASSUMED SHAPE OF FLOOD FRONT AFTER BREAKTHROUGH OF THE SWEPT REGION INTO A PRODUCING WELL OF A FIVE-SPOT PATTERN.

$$\text{where} \quad r_f = d \sqrt{\frac{2(1-E_s)}{\pi}} . \quad \text{ft} \quad\cdots (9)$$

After breakthrough, the flood front will be assumed to have the shape shown in Fig. 3.

The flow rate from each region is proportional to the mobility and to the angle open to flow from that region. This leads to the relation

$$\frac{a}{2\pi} = \frac{f}{f + M(1-f)} , \quad\cdots (10)$$

where f is the fraction of the producing stream from the swept region, and a is the angle (in radians) open to flow from the swept region.

With values of a from Eq. 10 and data of areal sweep vs fractional flow from the swept region, the injectivity after breakthrough is

$$R_{11} = \log \frac{r_{ei}}{r_{wi}} + \log \frac{r_{ep}}{r_f}$$

$$+ \frac{2\pi f}{a} \log \frac{r_f}{r_{wp}}$$

$$\frac{i}{p_{wi} - p_{wp}} = \frac{0.003076 \, h\lambda_s}{R_{11}} ,$$

$$\text{res B/D-psi} \quad\cdots\cdots (11)$$

$$\text{where} \quad r_f = d \sqrt{\frac{2(1-E_s)}{\pi(1-\frac{a}{2\pi})}} . \quad \text{ft} \quad\cdots (12)$$

When areal sweep vs fractional flow from the swept region is not known, an approximation of injectivity after breakthrough can be obtained by assuming the radius r_f to be constant and equal to the value obtained from Eq. 9 or Eq. 12 using the breakthrough value of areal sweep E_s. With a fixed radius r_f, the angle a determined by Eq. 10 also establishes areal sweep as a function of fractional flow from the swept region. Patterns for which areal sweep data are available show no significant difference between the injectivity calculated using areal sweep data and the injectivity calculated by fixing the radius r_f at the breakthrough value of areal sweep.

The approximate relative injectivities for the five-spot pattern calculated from Eqs. 4, 6, 8, 10 and 11 are shown in Figs. 4 and 5 for comparison with experimental data reported by Aronofsky, et al,[4] and by Caudle, et al.[5] The agreement is good except for very low mobility ratios where the effects of by-passing, fingering, and saturation gradient across the front become more pronounced. For these calculations, the value of r_{ei} was taken equal to r_{ep} for mobility ratios for which breakthrough occurs at areal sweeps of more than 50 per cent of the total area. For mobility ratios in which breakthrough occurred prior to 50 per cent areal sweep, the value of r_{ei} was calculated from the per cent areal sweep

at breakthrough as $r_{ei} = d\sqrt{\dfrac{2E_s}{\pi}}$, and the value of r_{ep} was calculated as $r_{ep} = \sqrt{\dfrac{2d^2}{\pi} - r_{ei}^2}$.

IRREGULAR WELL SPACING OR UNEQUAL PRODUCING RATES

The injectivity of a flood pattern with irregular well spacing or unequal producing rates can be estimated in a manner similar to that described for the five-spot by distributing the drainage area of the pattern among the producing wells. The area assigned to each of the wells is then approximated by radial- and linear-flow segments, and the progress of the front is traced through these segments.

Dividing the area among the producing wells first involves dividing the total area into isolated or separate elements (corresponding to the division of the five-spot into symmetrical elements) and, then, dividing this isolated element among the producing wells in the element.

One method of dividing the total area into isolated elements for separate treatment is to use as dividing lines the lines joining all the producing wells which are supplied by one particular injection well. Fig. 6 shows an isolated element obtained in this way. The centrally located injection well supplies four producing wells. Lines are drawn connecting each of these producing wells with its two neighbors, and these lines form an irregular polygon which is taken as an isolated element of the total flood area.

To distribute this isolated element among the producing wells, a point is located on the line
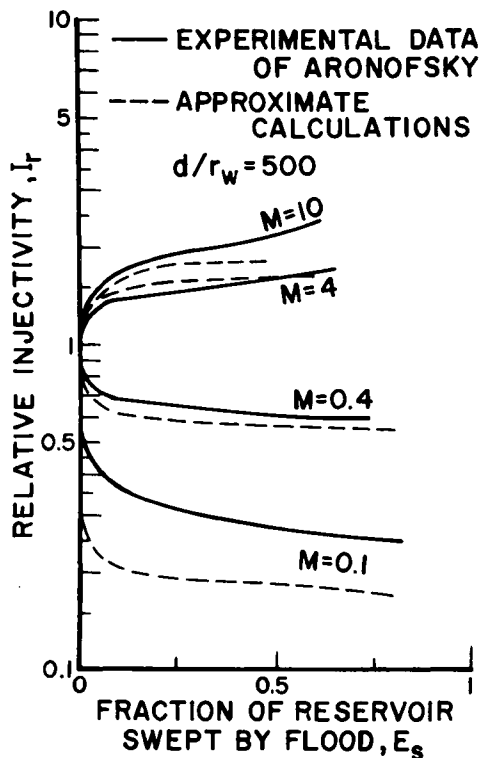
joining each pair of neighboring wells. This point divides the line between the wells in proportion to the total producing rates of the wells. In Fig. 6, for example, suppose that the total well rates have the following ratios: $q_1/q_2 = 1$, $q_2/q_3 = 5/4$, $q_3/q_4 = 8/9$, and $q_4/q_1 = 9/10$. Then four points are located as shown in Fig. 6, dividing the four sides of the irregular polygon into these ratios. Points are located at one-half the distance from Well 1 toward Well 2, five-ninths the distance from Well 2 toward Well 3, and so on.

Each of these individual well areas is now divided into radial segments, or possibly into radial and linear segments. The radius of the segment at the injection well, r_{ei}, can usually be taken as half the distance to the nearest producing well. A value of r_{ep} can then be calculated for each well so that the sum of the areas of the two radial sectors for each well is equal to the area assigned to that well.

The flood front is then traced through these sectors in a manner similar to that described for the five-spot. In the flood pattern of Fig. 6, for example, when the flood front is between the injection well and the radial boundary, r_{ei} (and prior to break-
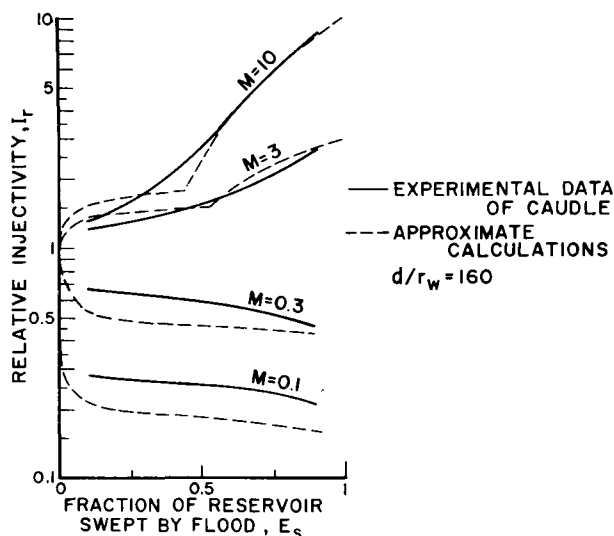

FIG. 5 — COMPARISON OF APPROXIMATE CALCULATIONS WITH EXPERIMENTAL INJECTIVITIES OF CAUDLE FOR FIVE-SPOT PRODUCING PATTERN.

FIG. 4 — COMPARISON OF APPROXIMATE CALCULATIONS WITH EXPERIMENTAL INJECTIVITY OF ARONOFSKY FOR FIVE-SPOT PRODUCING PATTERNS.
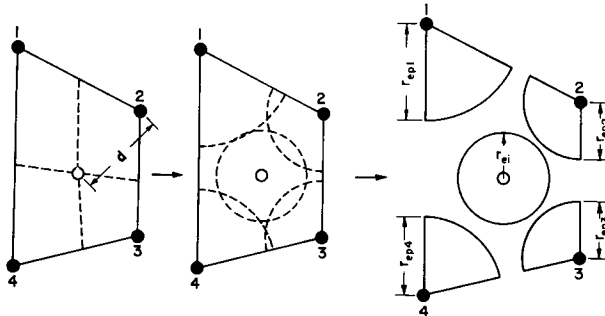

FIG. 6 — DIVISION OF IRREGULAR PATTERN INTO APPROXIMATING RADIAL-FLOW SECTORS FOR ESTIMATING INJECTIVITY.

through), the injectivity of the pattern referred to the difference in pressure between the injection well and producing Well 1) is

$$R_{13} = \frac{1}{M} \log \frac{r_f}{r_{wi}} + \log \frac{r_{ei}}{r_f}$$
$$+ \frac{q_1}{i} \log \frac{r_{ep1}}{r_{wp1}}$$

$$\frac{i}{p_i - p_{p1}} = \frac{0.003076 \, h\lambda_u}{R_{13}} \cdot \text{res B/D-psi}$$

$$\dots \dots \dots \dots \dots \dots \dots \dots (13)$$

Referred to the difference in pressure between the injection well and producing Well j, the injectivity of the pattern during the same period of the flood is

$$R_{14} = \frac{1}{M} \log \frac{r_f}{r_{wi}} + \log \frac{r_{ei}}{r_f}$$
$$+ \frac{q_j}{i} \log \frac{r_{epj}}{r_{wpj}}$$

$$\frac{i}{p_i - p_{pj}} = \frac{0.003076 \, h\lambda_u}{R_{14}}, \text{ res B/D-psi}$$
$$\dots \dots \dots \dots \dots \dots \dots \dots (14)$$

where

$i = \frac{1}{2\pi} \sum_{j=1}^{n} \theta_j q_j$, reservoir B/D,

n = number of producing wells in the pattern element ($n = 4$ in this example),

θ_j = vertex angle of the pattern boundary at producing Well j, radians,

q_j = total producing rate of Well j, reservoir B/D,

$r_f = \sqrt{\frac{E_s A_t}{\pi}}$, ft, and

A_t = total area of the isolated pattern element, sq ft.

When the flood front is between r_{ep} and the producing well, the injectivity is

$$R_{15} = \frac{1}{M} \log \frac{r_{ei}}{r_{wi}} + \frac{q_j}{i} \left[\frac{1}{M} \log \frac{r_{epj}}{r_{fj}} \right.$$
$$\left. + \log \frac{r_{fj}}{r_{wpj}} \right]$$

$$\frac{i}{p_i - p_{pj}} = \frac{0.003076 \, h\lambda_u}{R_{15}}, \text{ res B/D-psi}$$

$$\dots \dots \dots \dots \dots \dots \dots \dots (15)$$

where

$$r_{fj} = \sqrt{r_{epj}^2 - \frac{2q_j}{i} \left[E_s A_T - \pi r_{ei}^2 \right]}. \quad \text{ft}$$

$$\dots \dots \dots \dots \dots \dots \dots \dots (16)$$

After breakthrough occurs, the injectivity is

$$R_{17} = \log \frac{r_{ei}}{r_{wi}} + \frac{q_j}{i} \left[\log \frac{r_{epj}}{r_{fj}} \right.$$
$$\left. + \frac{2\pi f_j}{a_j} \log \frac{r_{fj}}{r_{wpj}} \right]$$

$$\frac{i}{p_i - p_{pj}} = \frac{0.003076 \, h\lambda_s}{R_{17}}, \text{ res B/D-psi}$$

$$\dots \dots \dots \dots \dots \dots \dots \dots (17)$$

where the radius r_{fj} after breakthrough can be assumed to be constant and equal to the value obtained from Eq. 16 using the breakthrough value of areal sweep, E_s. The angle open to flow from the swept region, a_j, can be calculated with Eq. 10.

The isolated element of a producing pattern can also be distributed among the producing wells by using the differences in pressure between the injection well and the producing wells as the criteria for assigning the radial-flow sectors to each producing well. Eq. 14 can be written for each producing well and the resulting equations solved for the appropriate values of r_{epj} according to the differences in pressure desired between the injection well and the producing wells. One method of doing this is by a simple iterative scheme. Eq. 14 can be written for each producing well and the results combined to give the total injection rate for the pattern as

$$i = \frac{\dfrac{0.003076 \, h\lambda_u}{2\pi} \displaystyle\sum_{j=1}^{J} \dfrac{\theta_j (p_i - p_{pj})}{\log \dfrac{r_{epj}}{r_{wj}}}}{1 + \dfrac{\log \dfrac{r_{ei}}{r_{wi}}}{2\pi} \displaystyle\sum_{j=1}^{J} \dfrac{\theta_j}{\log \dfrac{r_{epj}}{r_{wj}}}} \cdot$$

$$\text{res B/D}$$
$$\dots \dots \dots \dots \dots \dots \dots \dots (14a)$$

We begin by guessing the ratio of producing rates for all neighboring producing wells and calculating a set of r_{epj}'s as before. From Eq. 14a an approximate total injectivity is calculated. Substituting this injectivity into Eq. 14 gives an approximate producing rate for each producing well. The ratios of these producing rates can be used to re-divide the pattern and calculate a better approximation of the total injection rate. The initial guess is based only on the ratio of producing rates for neighboring producing wells and not on absolute rates. When the theoretical equations or model data for initial injectivities are available for unity mobility ratio, the actual injection rate (rather than the rate calculated from Eq. 14a) is used with Eq. 14 to re-divide the pattern area.

For comparison with experimental model data, the injectivity of a nine-spot pattern was calculated for an adverse mobility ratio of 10:1, and corner wells and side wells producing at equal rates. Although the nine-spot pattern generally is not considered to be an irregular pattern, it represents a system in which the producing wells are not all equidistant from the injection well. The injectivity was calculated from Eqs. 10, 14, 15, 16 and 17 by approximating the pattern area using two different criteria for determining the radii of the radial-flow sectors—(1) producing rates of the producing wells, and (2) the initial injectivities from the theoretical equations in Table 1.

The approximate calculations for the nine-spot are shown in Fig. 7, together with porous-model results[7] for the same conditions. The calculated injectivities show very close agreement with the model data. The disagreement at early areal sweep could be accounted for by wellbore damage in construction of the model. The slight disagreement in the two sets of model data is probably due to inhomogeneity in the model and extent of wellbore damage at the two corner wells of the model shown in Fig. 7.

BOUNDARY PATTERNS

To estimate the injectivities of boundary patterns, the effect of flow from outside the normal well network must be taken into account. A study of the boundary patterns listed in Table 1 showed that the effect of the position of the boundary on the injectivity of the outer row of wells approaches a limiting value when the boundary is more than one-half the well spacing beyond the outer row of wells, and it has almost no effect on wells two or more rows in from the boundary. All wells except the outer row thus can be treated as interior wells, and an estimate of injectivity in boundary patterns can be made by calculating an effective drainage angle θ for the outer row of wells and then tracing the

front advance as was done for the regular five-spot pattern. For example, if the five-spot pattern with all wells producing at the same rate were a boundary pattern as shown in Fig. 8, the injectivity of this boundary pattern could be estimated as follows.

The area of this pattern inside the well network can be approximated by radial-flow segments identical to those of Fig. 2. With these values of r_{ei} and r_{ep}, the assumed symmetry pattern is then represented by the radial sectors shown in Fig. 9.

Describing the flow in each sector by the radial-flow equation and combining gives an initial injectivity for this assumed-boundary symmetry element of

$$R_{18} = \log \frac{r_{ei}}{r_{wi}} + \frac{\pi q_b}{i\theta} \log \frac{r_{ep}}{r_{wp}}$$

$$\frac{i}{p_{wi} - p_{wpb}} = \frac{0.003076 \, h\lambda_u}{R_{18}},$$

res B/D-psi

$$\cdots \cdots \cdots \cdots \cdots \cdots \cdots \cdots \cdots (18)$$

where q_b = producing rate at the boundary well, reservoir B/D,

i = total injection rate of pattern, reservoir B/D, and

θ = effective drainage angle of boundary well, radians.

With all wells producing at the same rate, $q_b = (2/3)i$. With the injectivity by the approximate Eq. 18 set equal to the injectivity by the analytical equation in Table 1, the effective drainage angle θ can be calculated. For $d/r_w = 160$, the effective drainage angle θ in Fig. 9 is 2.05 radians. This effective drainage angle can be used in the radial flow equation, and the injectivity of this boundary pattern then can be estimated by tracing the front
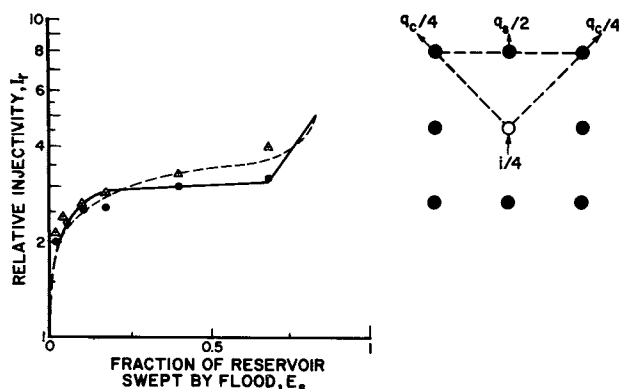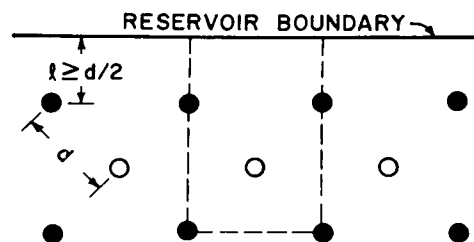

FIG. 7 — COMPARISON FOR ESTIMATED INJECTIVITY WITH EXPERIMENTAL DATA BY CAUDLE FOR A NINE-SPOT PRODUCING PATTERN ($M = 10$, $R = 1$, AND $d/r_w = 160$). CIRCLES AND TRIANGLES ARE EXPERIMENTAL INJECTIVITIES FOR THE TWO CORNER WELLS USED IN THE MODEL. DASHED LINE EQUALS CALCULATED INJECTIVITY WITH PATTERN AREA DIVIDED TO MAKE APPROXIMATE EQUATION MATCH THEORETICAL EQUATION AT $E_s = 0$. SOLID LINE EQUALS CALCULATED INJECTIVITY WITH PATTERN AREA DIVIDED IN PROPORTION TO PRODUCING RATES.

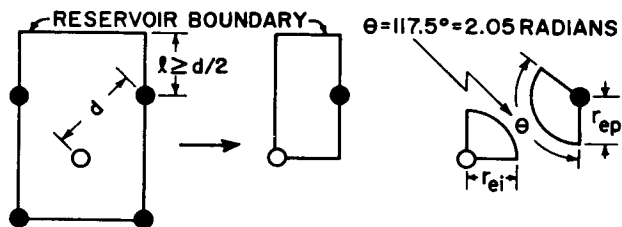FIG. 8 — BOUNDARY FIVE-SPOT PATTERN. DASHED LINE INDICATES ASSUMED SYMMETRY PATTERN.

FIG. 9 — DIVISION OF BOUNDARY FIVE-SPOT PATTERN INTO APPROXIMATING RADIAL SECTORS FOR ESTIMATING INJECTIVITY.

through these radial sectors in the same manner as was done for the interior five-spot pattern.

Based on the difference in pressure between the injection well and producing Well j, the injectivity of the five-spot boundary pattern of Fig. 9, prior to breakthrough and while the flood front is between the injection well and the boundary r_{ei}, is

$$R_{19} = \frac{1}{M} \log \frac{r_f}{r_{wi}} + \log \frac{r_{ei}}{r_f}$$

$$+ \frac{2\pi q_j}{i\theta_{jt}} \log \frac{r_{epj}}{r_{wj}}$$

$$\frac{i}{p_{wi}-p_{wj}} = \frac{0.003076\ h\lambda_u}{R_{19}},$$

$$\text{res B/D-psi}$$

$$\dots \dots \dots \dots \dots \dots \dots (19)$$

where $r_f = \sqrt{\dfrac{E_s A}{\pi}}$, ft,

A = total area within the normal well network, sq ft, and

θ_{jt} = total angle open to radial flow at Well j, radians.

While the flood front is between the boundary r_{epj} and the producing Well j, the injectivity is

$$R_{20} = \frac{1}{M} \log \frac{r_{ei}}{r_{wi}} + \frac{2\pi q_j}{i\theta_{jt}} \left[\frac{1}{M} \log \frac{r_{epj}}{r_{fj}} \right.$$

$$\left. + \log \frac{r_{fj}}{r_{wpj}} \right]$$

$$\frac{i}{p_{wi}-p_{wj}} = \frac{0.003076\ h\lambda_u}{R_{20}},$$

$$\text{res B/D-psi}$$

$$\dots \dots \dots \dots \dots \dots \dots (20)$$

where

$$r_{fj} = \sqrt{r_{epj}^2 - \frac{2q_j}{i\theta_{jt}} \left[E_s A - \pi r_{ei}^2 \right]},\ \text{ft}$$

$$\dots \dots \dots \dots \dots \dots \dots (21)$$

After breakthrough occurs, the injectivity is

$$R_{22} = \log \frac{r_{ei}}{r_{wi}} + \frac{2\pi q_j}{i\theta_{jt}} \left[\log \frac{r_{epj}}{r_{fj}} \right.$$

$$\left. + \frac{f_j\theta_{jt}}{a_j} \log \frac{r_{fj}}{r_{wj}} \right]$$

$$\frac{i}{p_{wi}-p_{wj}} = \frac{0.003076\ h\lambda_s}{R_{22}},\ \text{res B/D-psi}$$

$$\dots \dots \dots \dots \dots \dots \dots (22)$$

where

$$\frac{f_j\theta_{jt}}{a_j} = f_j + M(1-f_j),\ \dots \dots \dots (23)$$

and r_{fj} is assumed to remain constant after breakthrough and can be calculated from Eq. 21 using the value of E_s at the time breakthrough occurs at Well j.

Eqs. 19 to 23 are the general equations for estimating injectivity in complex well networks and reduce to the identical equations of the interior flood patterns given in previous sections for the five-spot infinite array and for the irregular interior patterns.

A comparison of the approximate injectivity of the boundary five-spot pattern of Fig. 9 with the injectivity of the interior five-spot pattern of Fig. 2 is shown in Fig. 10 for a mobility ratio of 10.

CONCLUSIONS

When the mobility of the fluid injected into a reservoir is different from the mobility of the reservoir fluid, the injectivity changes rapidly during the early part of the operation — and then only gradually until breakthrough occurs. Since most of the change in injectivity occurs during the early part of the flood while the flood front is nearly radial, reliable estimates of injectivity can be obtained by approximating the flood pattern with radial- and linear-flow segments.

Injectivity can be estimated after breakthrough by assuming that the flood front can be approximated by simple shapes and that the angle the swept region makes at the producing well is proportional to the rate of flow from the swept region. An estimate of breakthrough sweep efficiency is required to calculate injectivity after breakthrough.
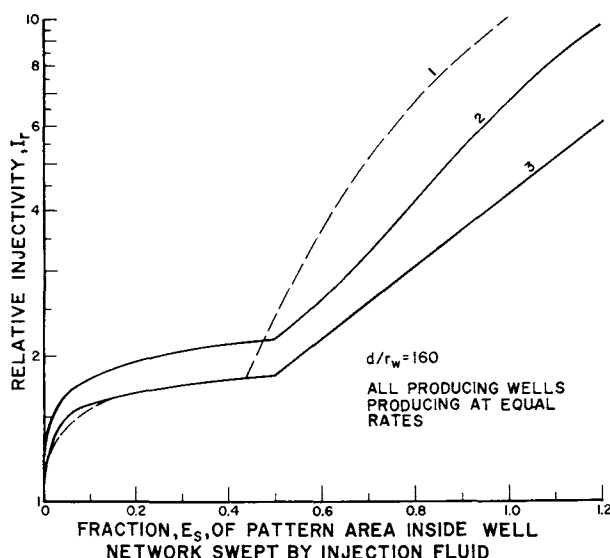

FIG. 10—COMPARISON OF RELATIVE INJECTIVITY OF (1) FIVE-SPOT INFINITE ARRAY WITH RELATIVE INJECTIVITY OF THE FIVE-SPOT BOUNDARY ARRAY OF FIG. 9 BASED ON (2) PRESSURE DIFFERENCE BETWEEN INJECTION WELL AND INTERIOR WELL AND (3) PRESSURE DIFFERENCE BETWEEN INJECTION WELL AND BOUNDARY WELL.

The approximate equations of injectivity can be applied to irregular interior patterns and to boundary patterns.

NOMENCLATURE

d = distance between injection and producing wells, ft

f = fraction of producing stream which is from the swept region

h = net pay thickness, ft

i = injection rate, reservoir B/D

k = specific permeability, md

p = pressure, psi

q = producing rate, reservoir B/D

r = radius, ft

E_s = fraction of reservoir swept by injection fluid

M = ratio of mobilities of swept region to unswept region

R = ratio of producing rates of corner well to side well for nine-spot producing pattern

a = angle open to flow from the swept region, radians

θ = vertex angle of pattern boundary at producing well, radians

λ = fluid mobility (k/μ), md/cp

μ = fluid viscosity, cp

SUBSCRIPTS

b = boundary well

e = external boundary

ei = external boundary of radial sector around injection well

ep = external boundary of radial sector around producing well

f = flood front

j = Well j

s = swept region

u = unswept region

w = well

wi = injection well

wp = producing well

ACKNOWLEDGMENT

REFERENCES

1. Muskat, M.: *Physical Principles of Oil Production*, McGraw-Hill Book Company, Inc., N. Y. (1949) 650.
2. Previously unpublished. A special case of the nine-spot equation was reported by Krutter, H.: "Nine-Spot Flooding Program", *Oil and Gas Jour.* (Aug., 1939) Vol. 38, 50.
3. Dyes, A. B., Caudle, B. H. and Erickson, R. A.: "Oil Production After Breakthrough — As Influenced by Mobility Ratio", *Trans.*, AIME (1954) Vol. 201, 81; also, original data on which this paper was based.
4. Aronofsky, J. S. and Ramey, H. J., Jr.: "Mobility Ratio — Its Influence on Injection or Production Histories in Five-Spot Water Flood", *Trans.*, AIME (1956) Vol. 207, 205.
5. Caudle, B. H. and Witte, M. D.: "Production Potential Changes During Sweep-Out in a Five-Spot System", *Trans.*, AIME (1959) Vol. 216, 446.
6. Prats, M., Matthews, C. S., Jewett, R. L. and Baker, J. D.: "Prediction of Injection Rate and Production History for Multifluid Five-Spot Floods", *Trans.*, AIME (1959) Vol. 216, 98.
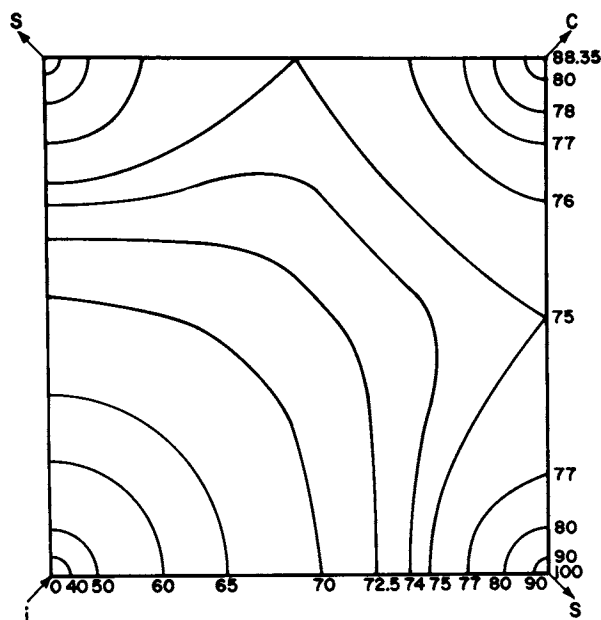7. Preliminary results from a model program now being

FIG. 11a—STEADY-STATE PRESSURE DISTRIBUTION IN NINE-SPOT PATTERN FOR UNITY MOBILITY RATIO AND CORNER-TO-SIDE PRODUCING RATIO = 0.5. (PER CENT OF TOTAL DIFFERENCE IN PRESSURE BETWEEN INJECTION WELL AND SIDE PRODUCING WELL.) d/r_w = 1,000.
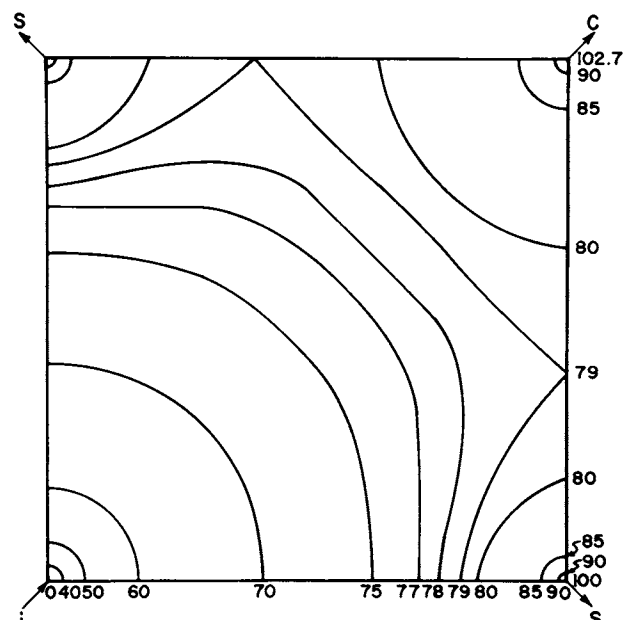

FIG. 11b—STEADY-STATE PRESSURE DISTRIBUTION IN NINE-SPOT PATTERN FOR UNITY MOBILITY RATIO AND CORNER-TO-SIDE PRODUCING RATIO = 1. (PER CENT OF TOTAL DIFFERENCE IN PRESSURE BETWEEN INJECTION WELL AND SIDE PRODUCING WELL.) d/r_w = 1,000.
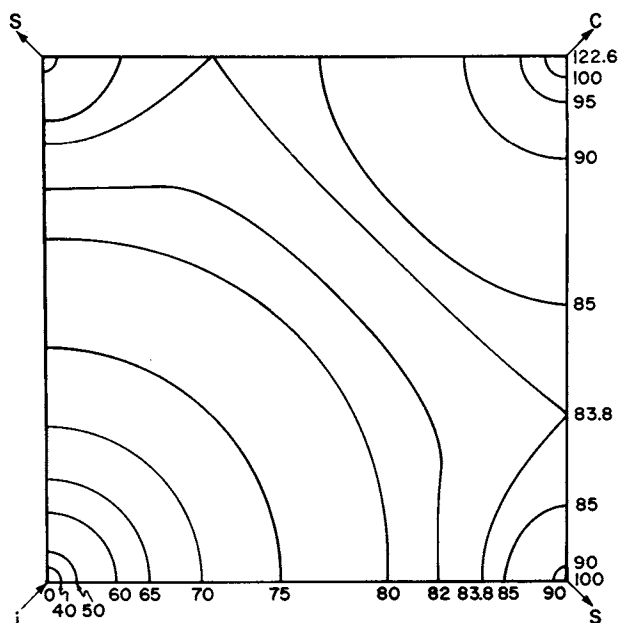
FIG. 11c—STEADY-STATE PRESSURE DISTRIBUTION IN NINE-SPOT PATTERN FOR UNITY MOBILITY RATIO AND CORNER-TO-SIDE PRODUCING RATIO = 2. (PER CENT OF TOTAL DIFFERENCE IN PRESSURE BETWEEN INJECTION WELL AND SIDE WELL.) $d/r_w = 1,000$.

carried on at the laboratory of The Atlantic Refining Co., Dallas.

8. Muskat, M.: "The Theory of Nine-Spot Flooding Networks", *Prod. Monthly* (March, 1948) 14.

APPENDIX

STEADY-STATE PRESSURE DISTRIBUTION IN THE NINE-SPOT PATTERN

The steady-state pressure distribution in the nine-spot pattern for unity mobility ratio was calculated after the method of Muskat[1,8] for ratios of corner-well to side-well production of 1/2, 1 and 2. For the infinite well array shown in Fig. 7, the steady-state pressure distribution is given by

$$H_k = \cosh \frac{\pi(y - kd)}{d} + \cos \frac{\pi x}{d}$$

$$H_k' = \cosh \frac{\pi(y - kd)}{d} - \cos \frac{\pi x}{d}$$

$$\frac{4\pi\lambda hp(x,y)}{i} = \frac{1}{2+R} \sum_{m=-\infty}^{m=+\infty} \ln \frac{H_{2m} H'_{2m+1}}{(H'_{2m})^2}$$

$$+ \frac{R}{2+R} \sum_{m=-\infty}^{m=+\infty} \ln \frac{H_{2m+1}}{H'_{2m}}, \quad \ldots\ldots\ldots\ldots\ldots(24)$$

where R = ratio of corner-well to side-well producing rates.

The calculated pressure distributions are shown in Fig. 11 as percentages of the total pressure difference between the injection well and the side well.

The singular point (discontinuity of pressure gradient) between the side well and the corner well was obtained by cross-plotting of the calculated pressure distribution and is only approximate. However, the large extent of the near-radial pressure distribution is readily apparent. In the case of $R = 1$ in Fig. 11, for example, more than 95 per cent of the pressure difference between the injection well and the corner well could adequately be described as radial. ★★★